Macromolecular Journals

Macromolecular Chemistry and Physics

Liquid-Glassy Polymer Interphases: Diffusion Kinetics in Conditions of Unlimited Liquid Supply

J. Pablo Tomba,* José M. Carella, Claudio J. Pérez, José M. Pastor

We investigate evidences of diffusion controlled by mechanical relaxation of the glassy matrix, i.e. Case-II mechanism, in a series of liquid/glassy interphases formed by PS and PPO as liquid and glassy components, respectively. Diffusion experiments were performed in conditions of unlimited supply of the liquid polymer, parallel to those in which Case-II has been effectively verified. Interphase profiles were obtained via optical sectioning with confocal Raman microspectroscopy (CRM). We observed that interphase diffusion kinetics were markedly Fickean, in contrast with interpretations from other authors that invoke Case-II to explain the mechanisms that rule interphase evolution in these systems.

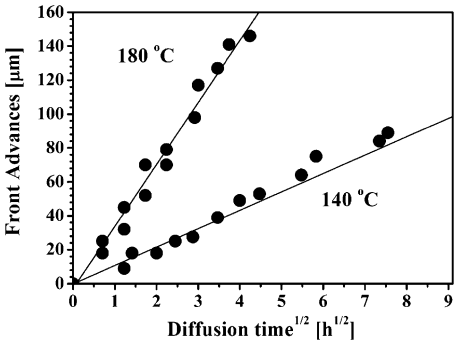

Introduction

When two miscible polymers with different glass transition temperature T_g are brought into intimate contact and heated to an intermediate temperature between their T_g, the sharp boundary between them gradually disappears and an interphase eventually evolves. The key characteristic of this process is that at the temperature of the experiment one of the polymers is in the melt state while the counterpart remains glassy, giving rise to a case of liquid-glassy polymer diffusion. This situation can be found in relevant fields of technology related with adhesion, welding, coating, laminating and control of transport/migration, among many others.

J. P. Tomba, J. M. Carella, C. J. Pérez
Institute of Materials Science and Technology (INTEMA), National Research Council (CONICET), University of Mar del Plata, Juan B. Justo 4302, (7600) Mar del Plata, Argentina
E-mail: jptomba@fi.mdp.edu.ar
J. M. Pastor
Department of Physics of Condensed Matter, University of Valladolid, Paseo del Cauce s/n, (47011) Valladolid, España

From a fundamental point of view, this diffusion case offers several mechanistic aspects that remain unclear. Recent publications in the primary literature exemplify quite well the existing controversy about the nature of the diffusion controlling step in these systems;[1,2] for more details see ref.[3] On the one hand, the concept of interphase evolution controlled by the mechanical relaxation of the glassy polymer, the core of the Case-II mechanism for diffusion of small penetrants in glassy matrices,[4,5] was proposed to explain the first liquid-glassy diffusion experiments on miscible polymer pairs.[6,7] In Case-II, the highly mobile small molecules penetrate and swell the glassy matrix, driven by osmotic suction,[8] up to reach a critical concentration that induces a swelling stress sufficient to cause yielding of the adjacent non-swollen glassy matrix. At this point, further penetration of small molecules in the non-swollen element is controlled by the time-dependent mechanical response of the glassy polymer, which gives rise to the particular features of Case-II, such as its anomalous diffusion kinetics or temperature dependence. In the opinion of other group of authors, Case-II cannot be operative in the case of *large* liquid molecules, such as bulky plasticizers, oligomers or polymers. They

DOI: 10.1002/macp.200800581

argue that the level of osmotic suctions generated by moderate-to-high molecular weight species, orders of magnitude lower than those associated with small molecules,[3] are not enough to overcome the plastic resistance of the glassy matrix and to initiate a diffusion mechanism by Case-II.[9] For these systems, they proposed a transport mechanism controlled by Fickean diffusion in a thin liquid layer adjacent to the glassy matrix; this layer is proposed to be formed from rapid dissolution of the glassy matrix by the liquid polymer, driven by the negative values of the thermodynamic interaction parameter commonly found in miscible polymer pairs.[9,10]

Conventionally, the studies of Case-II diffusion of small molecules in glassy matrices have been carried out in settings of *unlimited* penetrant supply, i.e. the polymer is in contact with an infinite reservoir with small molecules at constant concentration.[4,5] The theoretical machinery that describes Case-II has also been developed under this assumption; it describes well the linear sorption kinetics and apparent activation energies typically observed, markedly different to those that characterize the Fickean case.[4,5,8] On the contrary, a careful examination of the literature data shows that most part of experiments in liquid-glassy polymer systems has been carried out in conditions of *limited* supply of liquid polymer, i.e. a thin layer of liquid that diffuses in the glassy matrix.[1–3,6,7] Under the constraint of mass conservation, the concentration of liquid polymer throughout this thin layer depletes with diffusion time; therefore, local material properties behind the advancing diffusion front change continuously while diffusion evolves.[8] An example of this type of diffusion experiment is given in Figure 1, which shows front advances of liquid polystyrene (*l*-PS) in a glassy poly(phenylene oxide) (*g*-PPO) matrix, plotted in Fickean fashion as a function of $t^{1/2}$. The solid symbols correspond to experiments carried out by Tomba et al. using Confocal Raman Microspectroscopy (CRM, see below), for a sample held at 140 °C, well below the T_g of the glassy matrix (200 °C).[11] The inset shows the depletion in the volume fraction of PS (Φ^{PS}) throughout the liquid, as measured during the diffusion process, from its original value, 0.7, to about 0.4. The solid lines illustrate the expected $t^{1/2}$ and t scaling relationships characteristic of Fickean and Case-II regimes, the latter of which appears with an upward curvature in the Fickean plot. The marked departure showed by the experimental data from any of these models has been puzzling for several authors and illustrates in some way the complex diffusion kinetics that one may anticipate in systems evolving under changing driving forces, i.e. changing values of local concentration, osmotic suctions or T_g.[1,2,6a,7a]

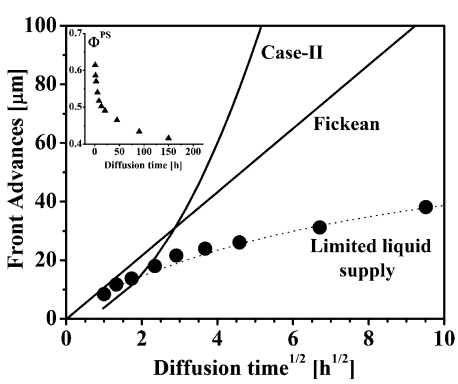

Figure 1. Diffusion kinetics in limited liquid supply experiments. Solid symbols refer to experimental data from ref. [11]; solid lines represent predictions from diffusion models. Inset: depletion of volume fraction of PS (Φ^{PS}) in the liquid layer during the diffusion process.

We believe that a more suitable approach for the study of the liquid-glassy polymer diffusion case, particularly justified if comparisons with well established transport models are going to be carried out, should include an investigation on diffusion kinetics in a setting of *unlimited* liquid polymer supply. As a step in this direction, we have undertaken a study of this type on a series of miscible polymer pairs with large difference in T_g between components: *l*-PS/*g*-PPO, *l*-PS/*g*-poly(α-methylstyrene) and *l*-poly(vinyl methyl ether)/*g*-PS. This paper reports the first results on the *l*-PS/*g*-PPO pair, for which diffusion mechanisms in apparent contradiction have been found.[1,2,12] Diffusion experiments were performed at temperatures well below T_g of the glassy PPO matrix and with PS samples of low molecular weight, for which relatively higher levels of osmotic suction, i.e. favorable conditions for Case-II, are expected. As experimental tool, we employed optical sectioning by CRM, a technique that directly measures local diffusant concentration and takes benefit of the natural spectroscopic contrast provided by the different chemical structures of PS and PPO. CRM is applied here in a novel configuration that delivers improved and steady depth resolution. It is shown that the Fickean view nicely describes the experimental observations and that Case-II features reported by other authors in this system are completely absent. To confirm these observations, we compare our results with predictions of a Fickean diffusion model for polymers in the melt state, which reproduces the main features of the experiments.

Experimental Part

The PS sample, referred to as PS0.7 ($\overline{M}_w = 740$ g·mol^{-1}, $\overline{M}_w/\overline{M}_n = 1.05$, $T_g = -5$ °C) was purchased from Polymer Source, while the PPO sample was obtained from Aldrich ($\overline{M}_w =$ 31 000 g·mol^{-1}, $\overline{M}_w/\overline{M}_n = 2.0$, $T_g = 212$ °C). The oil used as immersion fluid (B446082, $n = 1.5$) was purchased from Merck.

Macromol. Chem. Phys. **2009**, *210*, 359–366

DOI: 10.1002/macp.200800581

Polymer blends were prepared by freeze-drying benzene solutions at 10 wt.-% (w/w), in the presence of antioxidant (200 ppm, Santonox, Ciba-Geigy) to avoid polymer degradation during annealing. The high-T_g PPO-PS blend (glassy matrix, $T_g = 200\,^{\circ}C$) contains 95 wt.-% of PPO while the low-T_g PPO-PS blend (liquid layer, $T_g = 25\,^{\circ}C$) contains 70 wt.-% of PS.

A sketch of the experimental setup is shown in Figure 2. The samples for diffusion experiments, in a form of cylindrical specimens (6.5 mm diameter), were prepared by a sequential two-step process under vacuum, via a specially designed mold. First, a thin film of the high-T_g PPO-PS blend, about 200 μm thick, was molded at 40 °C above its T_g. The initial thickness of this layer was kept below the working distance of the objective (210 μm), which enabled us to see the original position of the glassy-liquid polymer interface and a wide span of depths to monitor interphase evolution inside the solid film. Next, an aluminum guard ring was placed and secured on top of that film. Finally, a thick layer of the low-T_g PPO-PS blend was vacuum molded on top of the high-T_g blend layer, in the cavity formed by the aluminum guard ring. The molding temperature of this second step was 70 °C, to minimize possible diffusion during sample preparation. To fulfill the condition of unlimited liquid supply, the liquid layer was about five times thicker than the glassy layer.

To promote polymer diffusion, samples were annealed in a temperature-controlled oven (±0.5 °C) under dry nitrogen atmosphere, for a period of time. They were then removed from the oven and quickly cooled to room temperature, which virtually stop interphase evolution, to be microscopically characterized. Raman spectra were recorded at room temperature, on a Raman microspectrometer DILOR LabRam Confocal, using a slit opening of 500 μm, a holographic grating of 1 800 lines · mm^{-1} and a confocal aperture of 200 μm. Samples were excited with a 16-mW He-Ne laser beam (632.8 nm wavelength). An immersion Olympus 100× [numerical aperture (NA) = 1.3, 210 μm working distance] microscope objective was used in the excitation and collection path. The nominal depth resolution in these instrumental conditions was 2.5 μm, as determined by measuring the response in z direction of a silicon wafer, a standard procedure in CRM.[13]

For optical sectioning, diffusion specimens were mounted on a microscope stage with controlled vertical displacement (z-axis), coupled to the Raman spectrometer. A drop of oil was placed between the glassy layer and the microscope objective just before confocal Raman profiling were carried out. The oil was exhaustively removed with tissue paper before sample annealing. Optical sections were obtained at various distances from the glassy layer surface by moving the focal plane along the z-direction (see Figure 2), resulting in a series of Raman spectra as a function of depth. The methodology used to obtain local concentration from the local Raman spectra has been described previously.[14]

Results and Discussion

We start briefly describing some details of the depth profiling mode employed to obtain the experimental data. In the past, we used optical sectioning by CRM with dry objectives, in a configuration where the optical axis was coincident with the diffusion direction;[1,3] the liquid/glassy polymer interphase was optically sectioned in the direction of the optical axis and through the relatively thin liquid layer (about 70 μm), in such a way that we measured the evolution of liquid polymer diffusion fronts as moving successively away from the microscope objective. In the present work, we choose the employment of immersion optics as a way to minimize refraction aberrations that penalize depth resolution.[13] In this configuration, the glassy-liquid polymer interphase is profiled through the solid layer, using the coupling oil on the less sensitive polymer of higher T_g, as shown in Figure 2. As optical sectioning is started from the oil/high-T_g polymer interface, we see the liquid fronts that develop as progressively advancing toward the microscope objective. The advantage of the latter approach, recently implemented in our lab for this type of experiments,[13] is that the depth resolution delivered by the instrument is improved by one order of magnitude and invariant with focusing depth. The analysis of diffusion profiles is now straightforward and avoids indirect calculations employed in earlier works.

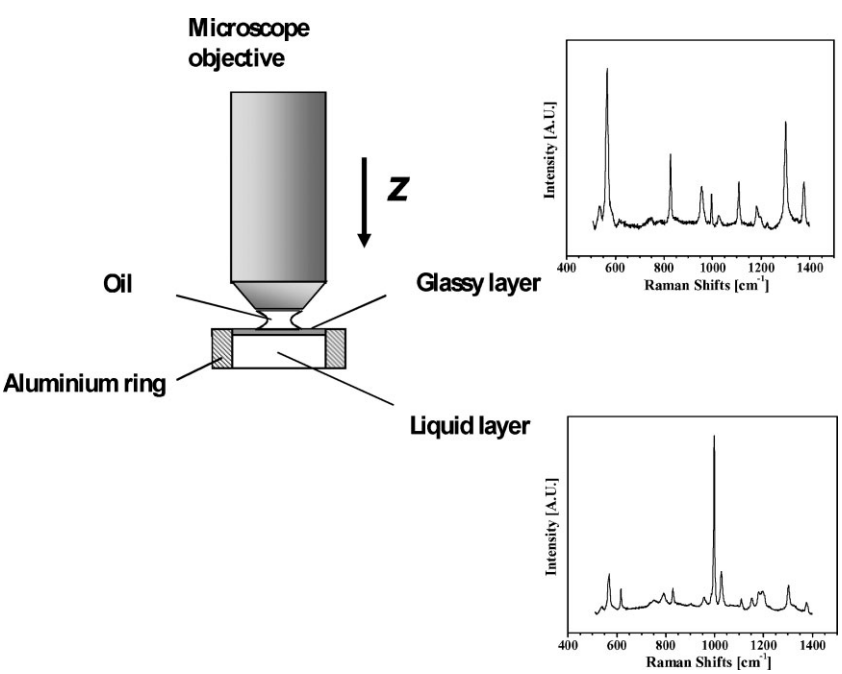

Figure 2. Schematic of the experimental setup used to measure diffusion profiles, where z represents the diffusion coordinate. Raman spectra of liquid and glassy layers show distinctive profiles that allows ready identification of individual distributions of polymer pair components along the z direction.

Figure 3A shows representative PS concentration profiles at *l*-PS/*g*-PPO interphases obtained by Raman micro-analysis along the diffusion direction. The profiles correspond to a sample held at 140 °C, 60 °C below the T_g of the PPO-rich matrix, for the diffusion times indicated in the plot. The zero in the depth axis corresponds to the oil/PPO-rich layer interface. In this coordinate system, the original *l*-PS/*g*-PPO interface should be seen at about 190 μm, dividing the glassy layer (0–190 μm), from the liquid layer (190–1 200 μm). The profiles show how the liquid PS diffuses into the PPO-rich glassy layer. They progressively advance in the form of sharp diffusion front, followed by a relatively flat region behind (larger depths). The inset of Figure 3A shows computer simulations of profile evolution, included to visualize the range of depths effectively examined, a value operationally restricted by the working distance of the microscope objective (210 μm). Notice that, as follows from computer simulations, the flat region extends over the whole thickness of the liquid film (about 1 000 μm, see below).

The shape of the profiles shown in Figure 3A reflects the large disparity in molecular mobility throughout the diffusion pathway. While sharp diffusion fronts advance toward the PPO-rich side in steps of few tens of microns, PPO molecules diffuse deeply into the PS-rich side, as revealed by the relatively uniform PS concentration behind the diffusion front. This asymmetric behavior is ascribed to the dramatic changes in free volume (and diffusivity) experienced by polymer molecules when passing from the low-T_g PS-rich region to the rich-PPO *glassy* side. Although PPO molecules travelled relatively large diffusion distances, well deep into the PS-rich side, they did not reach the external surface of that layer. This condition was confirmed by verifying invariance of PS concentration in the external part of the liquid layer. After each PS profile measurement, the composite specimen was placed upside-down on the microscope stage; then, the PS concentration was monitored over the first outer 200 μm of the liquid layer (1 000–1 200 μm range on the depth scale) with a "dry" objective. Figure 3B shows this type of data for a sample held at 180 °C for the times indicated, along with computer simulations in the inset, as a guide. We see that the PS concentration throughout this region did not deplete in the course of the experiment, remaining essentially constant, which verifies that what we are actually capturing is the *l*-PS diffusion from a source of basically invariant properties.

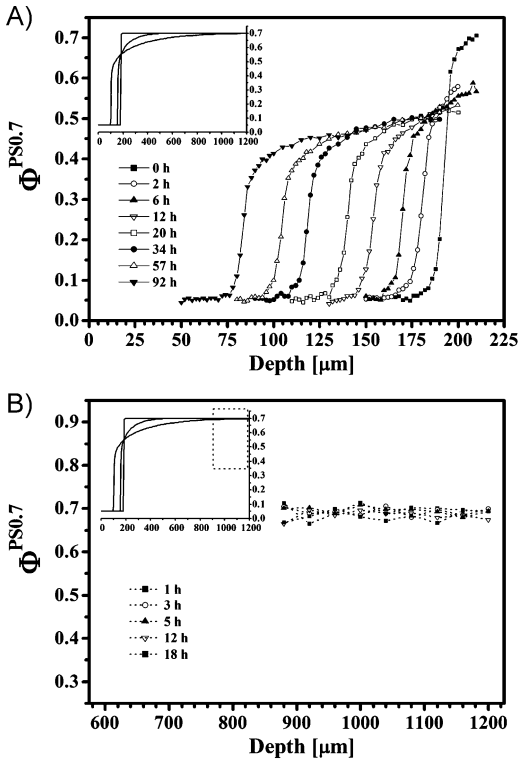

Figure 3. (A) Diffusion profiles of *l*-PS in a rich PPO glassy matrix under unlimited *l*-PS supply conditions. The data correspond to a sample held at 140 °C for the times indicated in the plot. (B) PS concentration at the external part of the liquid layer, for a sample held at 180 °C for the times indicated in the plot. Insets: *l*-PS diffusion profiles simulated by computer, as guideline; for details about the diffusion model, see ref. [9, 11]

In Figure 4 we present the advancing front kinetics in the context of Case-II and Fickean models. Figure 4A shows diffusion front advances as a function of elapsed diffusion time *t* for three of the temperatures studied, 140, 160 and 180 °C, all of them well below the matrix T_g (200 °C). A similar evolution pattern was observed in diffusion experiments conducted at 120 °C and 200 °C (not shown here). Figure 4B show the same data plotted in Fickean fashion. The position of the front on the diffusion coordinate was determined from the maximum in the derivative curve of the concentration profile. Notice the large amount of data collected and the wide range of diffusion times and temperatures spanned, compared with studies previously published in the literature on this system.[2]

We also characterized the temperature dependence of the diffusion process through values of apparent activation energy E_{df}. Details on the calculation of E_{df} from this type of data are given elsewhere.[1,7a] We plot first the successive positions of the advancing diffusion front (z_{df}) as a function of time for each of the diffusion temperatures. From this plot, instantaneous front velocities (V_{df}), as dz_{df}/dt, are then calculated and plotted in Arrhenius fashion. The slope of the curves yields E_{df}. Figure 5 shows this type of data for the present experiments (i.e. unlimited supply, solid symbols), from which we obtained $E_{df} = 93.6 \pm 2.1$ kJ·mol^{-1}, in the range 120–180 °C, independently of the stage of the diffusion process. In Figure 5, we have also included data obtained from diffusion

Macromol. Chem. Phys. **2009**, *210*, 359–366

DOI: 10.1002/macp.200800581

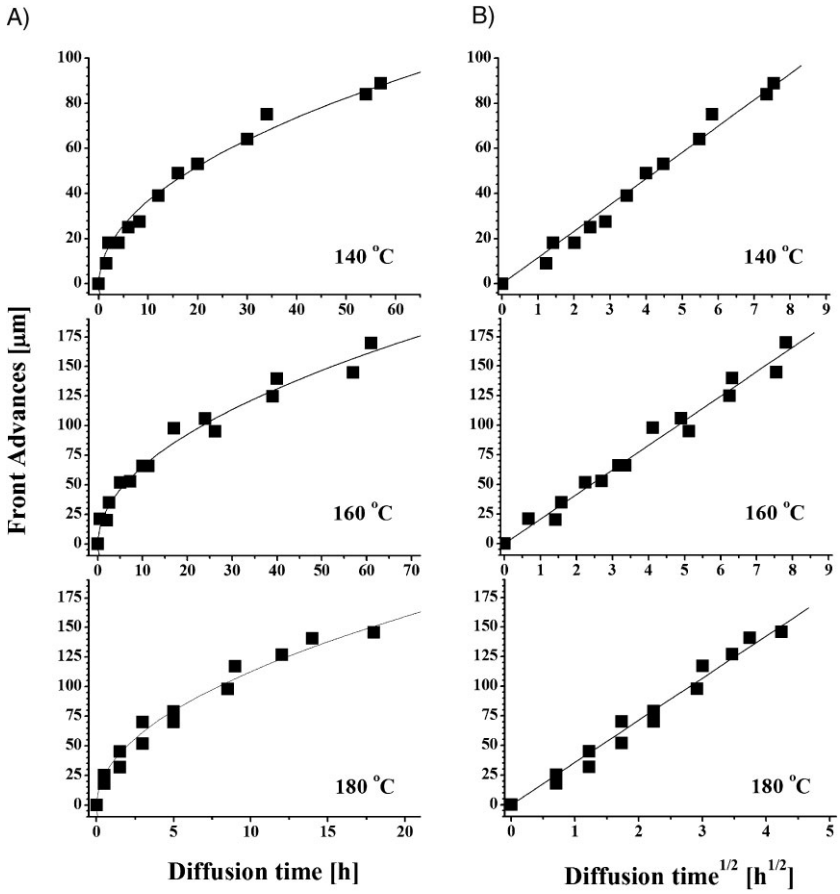

Figure 4. Apparent kinetics of the advancing diffusion fronts. Positions of *l*-PS fronts versus: (A) diffusion time; (B) square root of diffusion time. The solid symbols correspond to experimental data for the temperatures indicated; the solid lines represent linear fits to the data. Data collected correspond to at least two independent samples by temperature.

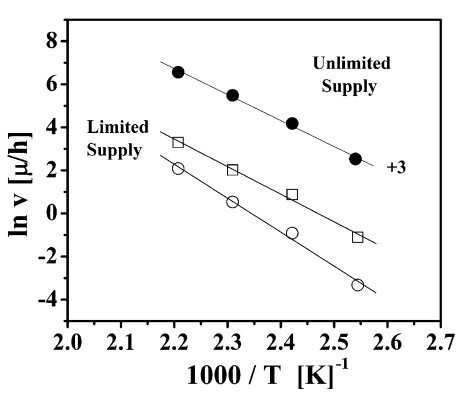

Figure 5. Plots of ln(V_{df}) against 1/*T* over the temperature range from 120 to 180 °C for the *l*-PS/*g*-PPO system. Solid symbols: unlimited supply experiments, shifted vertically by +3 units for visual clarity. Open symbols: limited supply experiments at $\Phi^{PS} = 0.6$ (squares) and at $\Phi^{PS} = 0.5$ (circles). The lines represent the linear fittings used to calculate E_{df}.

experiments under conditions of limited liquid supply, on the same system and on a similar temperature range, taken from ref.[11] (hollow symbols). In this setup, E_{df} has shown to be sensitive to the stage of the diffusion process considered; for this reason, E_{df} values were calculated and reported for specific values of PS concentration at the liquid side. The data shown correspond to E_{df} of 106.6 ± 3.8 kJ·mol^{-1} ($\Phi^{PS} = 0.6$) and 130.8 ± 3.8 kJ·mol^{-1} ($\Phi^{PS} = 0.5$).

Boundary Conditions and Apparent Diffusion Kinetics

The condition of infinite supply arises naturally from studies of penetration of small molecules into glassy polymers, when the piece of polymer is put in contact with a *large*, essentially invariant, source of simple liquids or vapors, i.e. the classic sorption experiments where the Case-II diffusion mechanism has been verified. The concept is embodied in the original models for Case-II developed by Hui and Kramer,[15] based on Thomas and Windle's ideas,[4] that predict front propagation at invariant velocity under the assumption of constant (equilibrium) concentration of penetrant in the plasticized layer preceding the advancing front. A more recent work of Argon emphasizes these ideas showing that diffusion front velocities increase sharply with concentration of small molecules in the plasticized layer, particularly in the concentration range slightly above the critical value necessary for Case-II initiation.[16] We then conclude that a necessary condition for observation of strictly linear diffusion kinetics under Case-II conditions is not only the coupling between diffusion and the mechanical relaxation of polymer segments but also the presence of a plasticized layer with invariant properties adjacent to the glassy matrix that supplies the small molecules.

In this context, and assuming that the condition of unlimited liquid supply is effectively satisfied in our diffusion experiments, we conclude from Figure 4A that our data on the *l*-PS/*g*-PPO system are definitively *not* consistent with a Case-II diffusion mechanism. The departure from a linear time scaling is systematic for the wide range of temperatures and times covered by our experiments. Conversely, the data from Figure 4B show an excellent agreement with the $t^{1/2}$ scaling law, character-

istic of a Fickean regime. Recent diffusion experiments carried out in our lab that explore diffusion kinetics at even lower diffusion temperatures (80–120 °C), unprecedented for this system, showed a similar time scaling law. Overall, these observations demonstrate unequivocally the neat Fickean character of the diffusion mechanism in the *l*-PS/*g*-PPO, ruling out the occurrence of Case-II.

The analysis of other features of the diffusion experiments supports the earlier statement. For instance, the response of diffusion rates to temperature is also consistent with the Fickean case. In Case-II, activation energies reflect the process of plastic deformation of the glassy polymer that controls the advance of the diffusion front,[17] with values typically higher than those that characterize pure Fickean diffusion.[4] The E_{df} value reported here, 93.6 $kJ \cdot mol^{-1}$, is far below that reported for plastic deformation of glassy PPO matrices measured by Creton, i.e. 230 $kJ \cdot mol^{-1}$ in a temperature interval between 15 and 150 °C below T_g.[11,18] The independence of E_{df} with the stage of the diffusion process appears consistent with the fact that PS concentration at the liquid side remains almost steady. The larger values for E_{df} obtained from limited supply experiments ($E_{df} = 106.6$ and 130.8 $kJ \cdot mol^{-1}$), correspond to later stages of the diffusion process that occur under lower Φ^{PS} values at the plasticized layer (or higher local T_g). This can be taken as an indication that the temperature interval between the experimental temperature and local T_g at the controlling step, plays a role, as predicted by the Williams-Landel-Ferry (WLF) equation. In fact, the whole sets of values lie well in the range of activation energies values for viscous flow predicted by WLF for this system.[1]

On the other hand, induction periods or Fickean precursors preceding the diffusion fronts, features typically found in Case-II, are absent. Over the induction period, a low concentration of the small molecules fill interstitial sites in the glassy polymer (free volume), generating the so-called Fickean precursors. This temperature-dependent stage elapses until the conditions for control by mechanical relaxation are established. Fickean precursors play a key role in plasticizing the glassy matrix, additionally reducing its yield stress and thus favoring Case-II initiation. Once conditions of control by Case-II are established, the diffusion front propagates with self-similarity, with the Fickean precursor ahead as a concentration tail. Examination of our data in Figure 4B does not reveal indication of an induction period, i.e. a delay in the propagation of the diffusion fronts, as all the plots pass well through the origin. Similarly, Figure 3A shows that the advancing liquid profiles are essentially sharp, with no discernible concentration tails; the rounding observed in the profile edges are most likely due to instrumental broadening.[13] One may argue that we are possibly missing the phenomenon due to the limited spatial discrimination of our technique and that Fickean tails may be present at submicron scale. At this point, we refer to previous work carried out by other research groups with techniques with higher spatial resolution (few nanometers), which have shown that the liquid/glassy polymer interphases are indeed sharp, with a thickness on the order of the radius of gyration of the molecules of the glassy layer.[2,11] Overall, the absence of Fickean tails reflects the low diffusivities one would expect for penetration of large-sized molecules through a pathway of interstitial holes;[3,5] consequently the efficiency of these molecules in decreasing the glassy matrix yield stress will be also low, which in turn penalizes the eventual initiation of control by Case-II.

Comparison of Interphase Kinetics with Model Predictions

As further support for these ideas, we compare the results of diffusion kinetics with predictions of well-established models for liquid-liquid polymer diffusion. The model used in the comparison describes the Fickean diffusion between two liquid polymers with different viscosity through the use of a concentration dependent diffusion coefficient. Full details of the model formulation can be found elsewhere.[9,11] Briefly, fluxes of individual polymers are expressed in the context of irreversible thermodynamics, where flux scales with the driving force for mass transfer, the chemical potential gradient of the given component, through a factor related with the intrinsic mobility of the diffusing molecule. To account for the dissimilar diffusivities of the components a bulk flow contribution is included in the transport equations. The thermodynamic factor (i.e. individual gradients of chemical potential) is derived from the Flory-Huggins theory, as a function of distributions of molecular weights for each component and the Flory-Huggins interaction parameter (χ) for the polymer pair. The kinetic factor (i.e. intrinsic polymer mobility) is in turn expressed in terms of the monomeric friction coefficients of each polymer and its blend composition dependence. Monomeric friction factors are typically available from independent tracer diffusion or rheological experiments. Changes in the monomeric friction coefficients with free volume are calculated with the WLF equation, using the local T_g as reference temperature. Local T_g values are adjusted point-by-point along the diffusion coordinate assuming that variations of T_g with blend composition are known.

We solved the model assuming Rouse-type dynamics for the liquid component. Thermodynamics of this polymer pair has been well characterized: the χ values found lie between −0.046 (120 °C) and −0.019 (200 °C).[19] Monomeric frictions coefficients for PS and PPO as a function of

DOI: 10.1002/macp.200800581

blend composition are also available.[20] As PS/PPO blends behave in thermo-rheological simple fashion, the same WLF scaling was used to describe the dynamics of both PS and PPO species for any blend composition.[20] The dependence of T_g with blend composition was determined independently from DSC experiments on homogenous PS/PPO blends, as reported earlier.[11]

It has already been shown that this physical model reproduces very well all the features of the diffusion profiles, predicting flat curves in regions of low viscosity (low-T_g side) and much steeper slopes when approaching to the solid matrix (high-T_g side). This marked asymmetry originates in the dramatic changes in monomeric friction coefficients along the diffusion coordinate predicted by WLF, in turn controlled by local T_g, as extensively discussed in previous work.[9,11] Some exemplary diffusion profiles, calculated with the model above-described, were included in the insets of Figure 3. Here, we emphasize the ability of the model to reproduce features of the diffusion kinetics under different conditions, as a way to confirm the Fickean character of the liquid polymer transport. Figure 6 shows front positions plotted in Fickean fashion for unlimited supply experiments performed at 140 and 180 °C (symbols), along with predictions of the Fickean diffusion model (solid lines). It has also been included experimental data corresponding to a limited supply experiment carried out at 140 °C. To calculate front advances from model predictions, we computed the maximum of the first derivative of the calculated profile, the same methodology employed to obtain front advances from the experimental data.

The model prediction follows with precision the evolution of front advances for the complete range of annealing times. The same good agreement was found for other temperatures studied. Moreover, the same model, with the same parameters, except for the relative thickness of liquid/glassy layers, reproduces nicely the evolution of front advances in limited liquid supply experiments. This success, particularly the effectiveness of the WLF scaling to describe the response of the system to temperature under different supply conditions, indicates that the controlling step of the diffusion process is placed at the liquid polymer-matrix interphase, at liquid polymers concentrations corresponding to a local T_g quite lower than the annealing temperature.[1] This description provides a context to explain the downward deviations in the Fickean plots systematically observed in limited supply experiments and shown in Figure 1:[1,3,11] the transport of PPO molecules toward the liquid layer increases the local T_g along the PS diffusion path, reducing the gap between the annealing temperature and the local T_g and thus slowing down the transport rate of the liquid component.

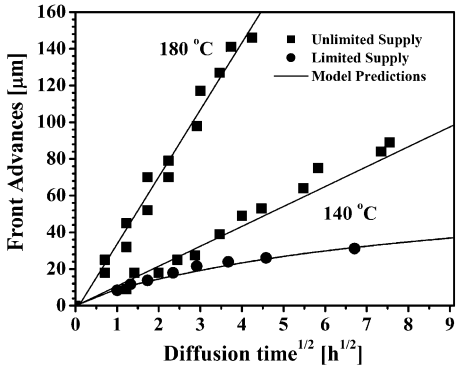

Figure 6. A comparison between experimental data and predictions of the Fickean model. Symbols correspond to experimental data while solid lines represent model predictions.

Conclusion

The evidence collected so far indicates that interphase evolution revealed by diffusion kinetics in the *l*-PS/*g*-PPO system is consistent with a diffusion mechanism with Fickean characteristics. No evidence in favor of control by Case-II was found. Overall, the response of the system to temperature appears compatible with a transport mechanism controlled by a liquid-liquid diffusion step rather than by a process of mechanical deformation of the glassy matrix, the central feature of Case-II.

Arguments against Case-II, based on recognizing that the molecular size of the penetrant plays as a decisive role in the occurrence of this diffusion mechanism,[3] has led us to assume that this picture of the process and the agreement found with the Fickean case is not particular to this polymer pair and represents a common feature in liquid-glassy polymer diffusion. Although more work is needed to definitively confirm these ideas, the results presented here, carried out in conditions where Case-II features should be easily discernible, constitute a solid first step in this direction.

Received: November 26, 2008; Accepted: December 2, 2008; DOI: 10.1002/macp.200800581

Keywords: computer modeling; confocal Raman microspectroscopy; diffusion; glass transition; melt

[1] L. Arzondo, J. P. Tomba, J. M. Carella, J. M. Pastor, *Macromol. Rapid Commun.* **2005**, *26*, 632.
[2] C. J. Lin, I. F. Tsai, C. M. Yang, M. S. Hsu, Y. C. Ling, *Macromolecules* **2003**, *36*, 2464.

[3] J. P. Tomba, J. M. Carella, J. M. Pastor, *Macromolecules* **2005**, *38*, 4355.
[4] [4a] N. L. Thomas, A. H. Windle, *Polymer* **1980**, *21*, 613; [4b] N. L. Thomas, A. H. Windle, *Polymer* **1981**, *22*, 627; [4c] N. L. Thomas, A. H. Windle, *Polymer* **1982**, *23*, 529.
[5] [5a] R. C. Lasky, E. J. Kramer, C.-Y. Hui, *Polymer* **1988**, *29*, 673; [5b] T. P. Gall, R. C. Lasky, E. J. Kramer, *Polymer* **1990**, *31*, 1491; [5c] T. P. Gall, E. J. Kramer, *Polymer* **1991**, *32*, 265.
[6] [6a] B. B. Sauer, D. J. Walsh, *Macromolecules* **1991**, *24*, 5948; [6b] E. Jabbari, N. A. Peppas, *Macromolecules* **1993**, *26*, 6229.
[7] [7a] P. F. Nealey, R. E. Cohen, A. S. Argon, *Polymer* **1995**, *36*, 3687; [7b] Q.-Y. Zhou, A. S. Argon, R. E. Cohen, *Polymer* **2001**, *42*, 613.
[8] A. S. Argon, R. E. Cohen, A. C. Patel, *Polymer* **1999**, *40*, 6991.
[9] J. P. Tomba, J. M. Carella, D. García, J. M. Pastor, *Macromolecules* **2001**, *34*, 2277.
[10] M. Geoghegan, R. A. L. Jones, M. G. D. Van der Grinten, A. S. Clough, *Polymer* **1999**, *40*, 2323.
[11] J. P. Tomba, L. Arzondo, J. M. Carella, J. M. Pastor, *Macromol. Chem. Phys.* **2007**, *208*, 1110.
[12] R. J. Composto, E. J. Kramer, *J. Mater. Sci.* **1991**, *26*, 2815.
[13] J. P. Tomba, J. M. Carella, J. M. Pastor, *Appl. Spectrosc.* **2006**, *54*, 1515.
[14] J. P. Tomba, *J. Polym. Sci., Part B: Polym. Phys.* **2005**, *43*, 1144.
[15] C.-Y. Hui, K.-C. Wu, R. C. Lasky, E. J. Kramer, *J. Appl. Phys.* **1987**, *61*, 5137.
[16] A. S. Argon, R. E. Cohen, A. C. Patel, *Polymer* **1999**, *40*, 6991.
[17] R. C. Lasky, E. J. Kramer, C.-Y. Hui, *Polymer* **1988**, *29*, 1131.
[18] C. Creton, J.-L. Halary, L. Monnerie, *Polymer* **1998**, *40*, 199.
[19] R. J. Composto, E. J. Kramer, D. M. White, *Macromolecules* **1988**, *21*, 2580.
[20] R. J. Composto, E. J. Kramer, D. M. White, *Polymer* **1990**, *31*, 2320.

DOI: 10.1002/macp.200800581